Surface effects on nanowire transport: a numerical investigation using the Boltzmann equation

Venkat S Sundaram and Ari Mizel

Department of Physics and Materials Research Institute, Pennsylvania State University, University Park, PA 16802, USA

E-mail: ari@phys.psu.edu

Abstract
A direct numerical solution of the steady-state Boltzmann equation in a cylindrical geometry is reported. Finite-size effects are investigated in large semiconducting nanowires using the relaxation-time approximation. A nanowire is modelled as a combination of an interior with local transport parameters identical to those in the bulk, and a finite surface region across whose width the carrier density decays radially to zero. The roughness of the surface is incorporated by using lower relaxation times there than in the interior.

An argument supported by our numerical results challenges a commonly used zero-width parametrization of the surface layer (Chambers 1950 *Proc. R. Soc.* A **202** 378). In the non-degenerate limit, appropriate for moderately doped semiconductors, a finite surface width model does produce a positive longitudinal magneto-conductance, in agreement with existing theory of Chambers. However, the effect is seen to be quite small (a few per cent) for realistic values of the wire parameters even at the highest practical magnetic fields. Physical insights emerging from the results are discussed.

(Some figures in this article are in colour only in the electronic version)

1. Introduction

The effect of a finite system size on the conductivity of a material is a subject of considerable physical interest, which has recently been lent added relevance and importance by rapid developments in nanowire synthesis and assembly [2–10], electrical characterization and transport measurement methods [5, 11–22]. The development of nanowires currently represents an important part of materials and applied physics research. Hierarchial self-assembly techniques [13] envisaged in semiconductor nanowires make them promising central elements of future integrated electronics.

Reports of basic functional two- and three-terminal semiconductor nanowire devices including junctions, bipolar transistors and field-effect transistors are now widely found in the literature. The nanoscale transport properties of several important semiconductors including Si [15, 16, 12, 5], GaAs [20], GaN [19] and Ge [23–25], and semi-metals [26–33] have been investigated in detail. (Bi has attracted great attention because of its unique combination of interesting properties and its potential for thermoelectric applications [28–35].) Bicrystalline nanowires [9], crossed nanowire structures [12], functional networks [13, 21, 17] including ultra-high-density lattices [17], heterostructures [36] and superlattice devices [20] are part of the rapidly growing body of novel nanowire configurations under development.

A central aspect of theoretical enquiry must be the extent to which the conductivity of a nanowire differs from that of the bulk material. At first glance, it seems reasonable to suppose that the conductivity is smaller in a nanowire because of the addition of surface scattering, assuming that the band structure does not change drastically. However, experimental results have yielded conflicting indications on this point, which is presently not well understood. Particularly intriguing are reports of mobility values higher than their bulk counterparts observed in silicon nanowires [18], while in other cases the mobility has been deduced to be orders of magnitude lower.

Such challenging theoretical questions, brought into immediate relevance by the extensive data on electrical transport in nanowires compiled in the last few years, make a thorough quantitative investigation valuable at this point. The widespread pursuit of experiments pertinent to the surface effect on conductivity motivates a generic numerical description of the finite-size effect allowing both freedom and simplicity in the incorporation of nanowire characteristics.

For large- and moderate-sized nanowires operated at room temperature, semi-classical kinetic effects are expected to be as important as quantum mechanical effects like the modification of band structure. Thus a semi-classical study is both necessary and desirable in the common regime where the diameter of the nanowires is much larger than the thermal wavelength. While a quantum mechanical approach is indispensable to investigate conductance in very narrow nanowires (radii of a few nanometres) [37, 38], it is neither viable nor suitable for larger nanowires with radii of the order of 100 nm. For the latter the use of the semi-classical Boltzmann equation is the appropriate method to approach a thorough quantitative study of finite-size effects.

These effects have previously been addressed theoretically only with simplistic assumptions regarding the surface. The analytical results most widely quoted are due to Chambers [1], who used kinetic-theoretical ideas to calculate the modification of the effective mean free path due to the presence of a surface and then used this value to find the conductivity. Essentially the same results were obtained using the Boltzmann equation with suitable boundary conditions in [39].

We present here the results obtained from a general numerical scheme we have developed to solve the Boltzmann equation in a cylindrical geometry. Such a direct numerical solution offers the requisite freedom in incorporating nanowire characteristics and conditions such as the equilibrium electron density profile, or the presence of defects and impurities. To retain conceptual simplicity, we employ the relaxation-time approximation as a first step towards the systematic modelling and prediction of nanowire conductivity with a view to relating model parameters to experimental data, and possibly casting a light on surface characterization [6, 40]. In this context, comprehensive experimental studies of Bi nanowires are of direct relevance [28, 31–33]. The introduction of diameter-controlled synthesis of nanowires [8, 6] provides yet another fruitful context for our study.

We emphasize that surface scattering is just one of many scattering mechanisms that contribute to the resistivity of a nanowire; other mechanisms, especially acoustic phonon

scattering, can be produce more dissipation in many circumstances. In addition, for studies of specific nanowires with specific surface defects and impurities, the relaxation time approximation employed here would ideally be replaced by a more exact approach such as Monte Carlo or quantum mechanical simulation as mentioned above. Our intention, however, is to contribute generic intuition about the behaviour of surface scattering in large wires, even when the specific surface scattering centres are unknown and even when other resistive effects may be primary. For this reason, we use a generic relaxation time approach and map out its predictions for varied choices of wire characteristics. Despite its approximate character, this approach confers useful insight and is substantially more refined than the often-invoked 'specularity coefficient' model [1, 39].

Inter alia, the results yield insights into the general problem of transport with a nominal relaxation time that varies with spatial coordinates, which is non-trivial because of the fact that the diffusion of carriers connects different spatial regions, making their properties interdependent, and thereby introduces a connectivity to the physical situation. This may be of direct relevance to transport in layered media such as magnetic multilayers [41–44].

The numerical problem resulting from a finite-difference representation of the Boltzmann equation with a simple grid is solved using the conjugate-gradient method, which offers significant computational efficiency. A comparison with analytical results in limiting cases confirms the reliability of the scheme.

The paper is organized as follows. In section 2 we describe our computational framework, and the form of the Boltzmann equation adapted to the problem at hand. Our surface model is described in section 3. We present our results in the simple case of zero magnetic field in section 4, showing how they conform to physical expectation, thus validating the numerical scheme used. The important limit of zero-width surface is considered in section 5. Section 6 is devoted to the longitudinal magneto-conductance arising due to the surface effect and is followed by a summary (section 7).

2. Boltzmann equation and problem specification

In our approach, we consider a cylindrical conductor which has a finite surface width, so that there is no abrupt change at the boundary to be dealt with through boundary conditions. In particular, this includes treating the unperturbed (i.e. when the external fields are zero) distribution function f_0 as a function of both space and momenta. In order to use the Boltzmann equation with such a distribution function f_0 we introduce an effective internal electric field $\mathbf{E_c}(\mathbf{r})$ in addition to any external field, to account for this spatial variation of f_0. In a confined cylindrical system where f_0 decays from its interior magnitude to zero over a finite surface width, the force due to this internal field is exactly analogous to the constraining force that keeps a particle within an enclosure with an abrupt boundary, and is therefore physically expected. With this additional internal field, the Boltzmann equation [45] for the distribution $f(\mathbf{p}, \mathbf{r})$ of non-interacting carriers in the relaxation time approximation with a spatially varying relaxation time is

$$\nabla f \cdot \frac{\mathbf{p}}{m} + \nabla_{\mathbf{P}} f \cdot q \left(\mathbf{E} + \mathbf{E_c} + \frac{\mathbf{p}}{m} \times \mathbf{B} \right) = -\frac{f - f_0}{\tau(\mathbf{r})}. \tag{1}$$

Here $\mathbf{E}$ and $\mathbf{B}$ are the external electric field and magnetic field, and q and m are the charge and mass of each carrier. It is convenient to introduce the deviation $\phi(\mathbf{p}, \mathbf{r}) = f(\mathbf{p}, \mathbf{r}) - f_0(\mathbf{p}, \mathbf{r})$ due to the presence of the external fields; the equation for ϕ is

$$\phi = -\tau(\mathbf{r}) \left[\nabla \phi \cdot \frac{\mathbf{p}}{m} + q \nabla_P \phi \cdot \left(\mathbf{E} + \mathbf{E_C} + \frac{\mathbf{p}}{m} \times \mathbf{B} \right) + q \nabla_P f_0 \cdot \left(\mathbf{E} + \frac{\mathbf{p}}{m} \times \mathbf{B} \right) \right]. \tag{2}$$
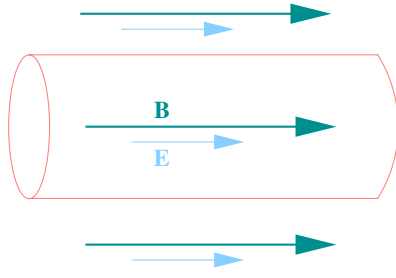
Figure 1. Model geometry.

We consider a long cylinder with no azimuthal or axial inhomogeneity and confine attention to the case where the external fields are uniform and parallel to the axis of the wire, defining a natural axis $\hat{z}$ of reference: $\mathbf{E} = E\hat{z}$; $\mathbf{B} = B\hat{z}$ (see figure 1).

Thus the physical problem at hand requires only one spatial degree of freedom $r = \sqrt{x^2 + y^2}$, although we have to treat all the momentum components. It is convenient to work with the local momentum components $p_r = \mathbf{p} \cdot \hat{r}$ and $p_\theta = \mathbf{p} \cdot \hat{\theta}$ rather than the canonical momenta in a cylindrical system, because the canonical momentum conjugate to θ is an angular momentum. Also, to preserve form (2) of the Boltzmann equation, f, f_0 and ϕ are defined as coordinate densities in the space of (p_r, p_θ, p_z, r) so that $f \, dp_r \, dp_\theta \, dp_z \, dr$ is the number of carriers in a volume element of this space. The missing volume element factor $2\pi r$ is absorbed into f, changing the internal field E_c, as we shall see. We solve equation (2) by discretizing on a real space grid of about 20^4 grid points. The resulting matrix equation is solved by the method of conjugate gradients.

The drift velocity, which is the population average of the component of the carrier velocity parallel to the external electric field, is

$$\langle v_z \rangle = \frac{\langle p_z \rangle}{m} = \frac{1}{m} \frac{\int d^3 p \, dr \, f(\mathbf{p}, r) p_z}{\int d^3 p \, dr \, f(\mathbf{p}, r)} = \frac{1}{m} \frac{\int d^3 p \, dr \, \phi(\mathbf{p}, r) p_z}{\int d^3 p \, dr \, f_0(\mathbf{p}, r)}. \tag{3}$$

The effective conductivity σ is $q\langle v_z \rangle N / l\pi r^2$, where N is the total number of carriers in the wire, l is its length and πr^2 its cross-sectional area.

An explicit expression for E_c can be directly deduced from the spatial variation of f_0 for an arbitrary form of the latter, since by definition of the unperturbed distribution,

$$\nabla f_0 \cdot \frac{\mathbf{p}}{m} + \nabla_{\mathbf{P}} f_0 \cdot q\mathbf{E_c} = 0. \tag{4}$$

For simplicity, we assume that the spatial dependence of the distribution function is completely separable from the momentum dependence so that $f_0 = F(\mathbf{p})\xi(\mathbf{r})$ and the internal field $\mathbf{E_C}$ points only in the direction of r: $\mathbf{E_C} = E_C(r)\hat{r}$. The computational results described below pertain to the case where the momentum-distribution is Maxwellian:

$$F(\mathbf{p}) = \exp\left(-\frac{p^2}{2mkT}\right). \tag{5}$$

Inserting $f_0 = F(\mathbf{p})\xi(r)$ and (5) in (4) we see that the simplest consistent form of the internal field is

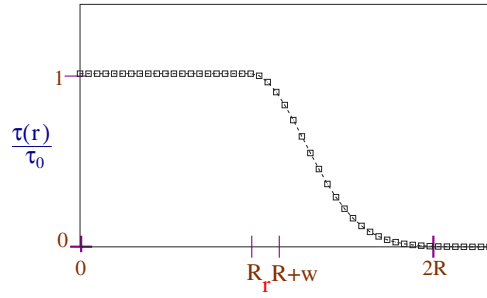$$E_c(r) = \frac{kT}{q} \frac{1}{\xi(r)} \frac{d\xi}{dr}. \tag{6}$$

Figure 2. Radial profile of the relaxation time $\tau(r)$.

3. Surface model

We use a simple, continuous model to include the effects of the surface on the conductivity. The fact that there are no carriers beyond the wire radius is accounted for by taking the volume density of carriers to decay spatially as a Gaussian with a width w beyond a certain radius r_0. A Gaussian function is chosen because of its mathematical simplicity and because its qualitative form is physically reasonable—we anticipate qualitatively valid physical conclusions using this form. The inhomogeneous carrier density results from a constraining electric field that is proportional to the difference $r - r_0$ for $r > r_0$ and is directed towards the wire axis. An additional term proportional to $1/r$ in the effective internal field E_c arises on using equation (6) due to the inclusion of the volume factor $2\pi r$ in the definition of f, as mentioned in section 2.

$$f_0 = F(\mathbf{p})\xi(r) = \begin{cases} r \exp\left(-\dfrac{p^2}{2mkT}\right) & r < r_0 \\[2mm] r \exp\left(-\dfrac{(r - r_0)^2}{2w^2}\right) \exp\left(-\dfrac{p^2}{2mkT}\right) & r \geqslant r_0 \end{cases} \tag{7}$$

$$E_c(r) = \frac{kT}{qr_0}h(r) = \begin{cases} \dfrac{kT}{qr} & r < r_0 \\[2mm] \dfrac{-kT(r - r_0)}{qw^2} + \dfrac{kT}{qr} & r \geqslant r_0. \end{cases} \tag{8}$$

We take w to be of the order of $0.1 \times R$ and consider the effect of varying its value in section 5.

The relative roughness of the surface is described by lower relaxation times $\tau(r)$ past a radius R. The key property of the surface that we seek to capture is that the material there has a substantially lower collision time than the bulk. We also want the $\tau(r)$ to vary smoothly. Further, it is reasonable that the change of character is monotonic in radial values. We choose a Gaussian decay form with a width w_r

$$\tau(r) = \tau_0\chi(r) = \begin{cases} \tau_0 & r < R \\[2mm] \tau_0 \exp\left(-\dfrac{(r - R)^2}{2w_r^2}\right) & r \geqslant R \end{cases} \tag{9}$$

because it is a simple single expression with these three properties. The radial profile of the relaxation time is shown in figure 2. It is not essential *a priori* that $\xi(r)$ in equation (7) and $\tau(r)$ necessarily be assigned the same analytical form: this is merely an assumption of convenience, given the similar qualitative criteria that they satisfy. Further, the widths characterizing the two decays, w_r and w, are a pair of independent parameters, as are the radial values R and r_0

marking the onset of the respective decays. Thus, in principle, a study using our model would have to include the complete variation of two (dimensionless) variables,

$$A = \log\left(\frac{w_r}{w}\right) \qquad \text{and} \qquad D = \frac{(R - r_0)}{w_r}. \qquad (10)$$

It turns out that this does not significantly add to the physical information derived from the simplest case where the radii satisfy $R = r_0$ and also the widths $w = w_r$ (i.e. $A = D = 0$). We therefore focus on this simplest case and indicate where appropriate the consequences of making A and D non-zero.

4. Conductivity

In the absence of a magnetic field, it is possible to make certain predictions analytically about the behaviour of the conductivity. We work in the limit where E is small, so that the drift velocity $\langle v_z \rangle$ is always small in comparison to the thermal mean velocity v_{th}. If $\tau(r)$ were a constant, τ_0, the drift velocity would be given by the familiar result

$$\langle v_z \rangle = \frac{qE\tau_0}{m}. \qquad (11)$$

When τ acquires a non-trivial radial profile $\tau(r)$, its overall scale determines to what extent thin cylindrical layers at different radii affect their neighbours because of the diffusion of carriers from layer to layer. If this scale is so small that the mean free path of particles with velocities of the order of v_{th} is much smaller than the length scale ζ over which τ changes significantly (i.e. $\tau(r)v_{\text{th}} \ll \zeta = w$), the spatial connectivity is negligible, and one may treat the different layers separately. In this case, one can define an effective relaxation time τ_{geom} which depends only on the geometrical distribution of the relaxation time weighted by the relative carrier concentration $\xi(r)$ from equation (7).

$$\tau_{\text{geom}} = \frac{\int \mathrm{d}r \, \xi(r)\tau(r)}{\int \mathrm{d}r \, \xi(r)}. \qquad (12)$$

The use here of $\xi(r)$, which is the spatial factor in the unperturbed distribution function f_0, is consistent with the fact that the relaxation timescale is small. For the model discussed in section 3, this can be expressed simply in terms of the ratio $\omega = w/R$, providing a useful test for the numerical scheme in the limit of small τ_0.

$$\tau_{\text{geom}} = \tau_0 \frac{1 + \sqrt{\pi}\omega + \omega^2}{1 + \sqrt{2\pi}\omega + 2\omega^2}. \qquad (13)$$

It is therefore useful to consider the essential surface effect as the departure of the actual drift velocity for the nanowire as a whole from the value derived by inserting τ_{geom} in place of τ_0 in (10). This, as we have just observed, will be perceptible only when $\tau_0 v_{\text{th}}$ is comparable to the surface width, and significant only when comparable to the wire radius.

We can study the physical consequences of independently varying the surface widths and radii so that the A and D, given by equation (10), are non-zero. For large positive A, the relaxation time varies gradually across the wire so that the drift velocity saturates towards the geometric value $q\tau_{\text{geom}}E/m$ regardless of D. This is expected because a slow variation of $\tau(r)$ makes the effect of the inhomogeneity insignificant. If, further, D itself is non-negative this geometric value approaches the bulk value. As A decreases, so that w_r becomes a smaller factor of w, finally down to small fractions of it, the drift velocity departs more and more from the geometric value.
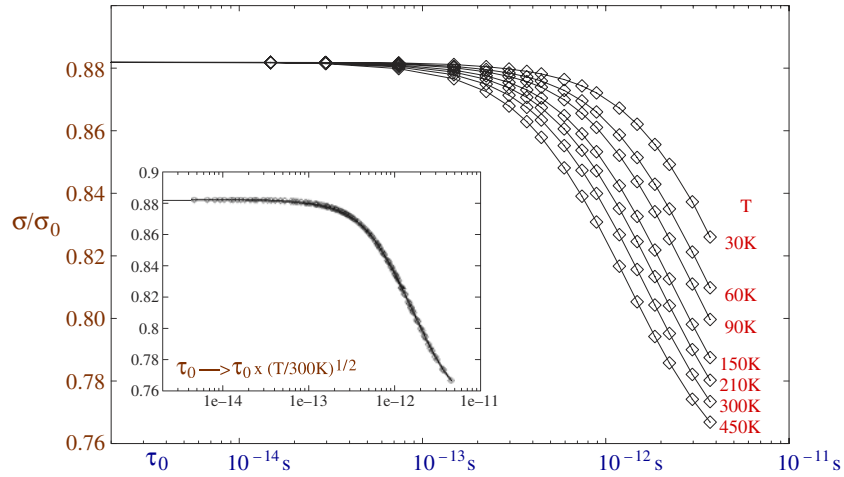
Figure 3. Relative conductivity as a function of the relaxation timescale τ_0 for different temperatures. σ_0 is the bulk value of the conductivity corresponding to a constant relaxation time τ_0. The inset shows the data collapse resulting upon scaling τ_0 by a factor $\sqrt{T/T_0}$. The fixed parameters are $E = 26\ \mathrm{kV\ m^{-1}}$, $R = 200\ \mathrm{nm}$ and $w = 40\ \mathrm{nm}$.

As $D \gg 1$ the drift velocity saturates at the bulk value regardless of A because hardly any carrier population exists beyond the point where the relaxation time begins to fall. As D decreases from positive to negative values, the drift velocity departs more and more from the geometric estimate. This is because the slope in the profile of $\tau(r)$ moves towards regions of higher population, thus affecting more carriers. A systematic variation of A and D on a grid of values yields numerical results that confirm the above conclusions. Significantly, the actual drift velocity is always lower than the geometric estimate.

It is important to note that the effect of spatially varying τ in a conductor as a whole is asymmetric in its action, between smooth (high τ) and rough (low τ) regions. A rough region is much less affected by the gradient of $\tau(r)$ in its neighbourhood than a smooth region. This is precisely because spatial connectivity is enhanced where $\tau(r)v_{\mathrm{th}}$ is large, as explained previously. Thus, in a conductor which has both regions of high τ and low τ, the latter separately exhibit geometric (unconnected) behaviour, showing no effect of the presence of the former.

But the effect of spatial variation on regions with high τ is to decrease mobility there, since carriers there can move enough to sample a significantly rougher region. Therefore, the effect of spatial variation on rough regions being negligible, its effect on a conductor as a whole, too, is a decrease in mobility. This consideration will later appear prominently in explaining the magneto-conductive effect as well (section 6). Figure 3 shows the variation of the conductivity as a function of the relaxation timescale for different temperatures. The ratio of the surface width to the wire radius ω is fixed at 0.2. As $\tau_0 \to 0$, the conductivity tends to the same fraction of the bulk value at all temperatures, which is seen to be almost exactly equal to the geometric factor 0.8815, the value obtained by putting $\omega = 0.2$ in equation (12). At higher temperatures, the departure from this ratio is also higher. This is physically expected since a higher temperature makes available higher radial velocities to the carriers in their random motion between collisions, thus increasing the communication between different layers. Thus we see that even if the relaxation time were independent of the temperature, the conductivity would have a temperature dependence in the low field limit because of the surface effect. Note

that to isolate the surface effect, the complex temperature variation of relaxation time in a real medium is deliberately suppressed, though it can be included easily in the computational scheme.

Further, it is seen in the inset that the data can be collapsed onto a single curve by using the transformation $\tau_0 \to \tau_0\sqrt{T/T_0}$, where T_0 is an arbitrary temperature. In other words, when $B = 0$ the temperature is a reducible parameter in the limit of a low electric field, which can be accounted for exactly by rescaling τ in proportion to the corresponding mean thermal velocity. This can be seen analytically by direct use of the Boltzmann equation, through a transformation to dimensionless variables. Rewriting equation (2) with the functional forms in (7)–(9) we have

$$\phi + qE\tau(r)\frac{\partial\phi}{\partial p_z} + \frac{kT}{R}h(r)\tau(r)\frac{\partial\phi}{\partial p_r} + \tau(r)\frac{p_r}{m}\frac{\partial\phi}{\partial r} = \frac{qE\tau(r)p_z}{mkT}\mathrm{e}^{-p^2/2mkT}\xi(r). \tag{14}$$

Now introducing the variables $\mathbf{u} = \mathbf{p}/\sqrt{mkT}$ and $s = r/R$, we get

$$\phi + \frac{qE\tau_0}{\sqrt{mkT}}\chi(s)\frac{\partial\phi}{\partial u_z} + h(s)\frac{\tau_0}{R}\sqrt{\frac{kT}{m}}\chi(s)\frac{\partial\phi}{\partial u_r} + \chi(s)u_r\frac{\tau_0}{R}\sqrt{\frac{kT}{m}}\frac{\partial\phi}{\partial s}$$
$$= \frac{qE\tau_0\chi(s)\xi(s)u_z}{\sqrt{mkT}}\mathrm{e}^{-u^2/2}. \tag{15}$$

When E is small, ϕ is of the same order of smallness, and therefore the second term in the left-hand side of (14) is negligible. This leaves us with a linear differential operator containing τ_0 only in the combination $\tau_0\sqrt{T}$ acting on ϕ in the left-hand side. The appearance of τ_0 and T in the right-hand side (inhomogeneous term) of course merely alters the overall scale of ϕ. Hence the function $\phi(\mathbf{u}, r)$ may be written as $\frac{qE\tau_0}{\sqrt{mkT}} \times H(\mathbf{u}, s; \tau_0\sqrt{T})$, where H is the solution of (14) with the constant $\frac{qE\tau_0}{\sqrt{mkT}}$ absent in the right-hand side. The drift velocity is

$$\langle v_z \rangle = \sqrt{\frac{kT}{m}}\frac{\int \mathrm{d}^3u \int \mathrm{d}s\, u_z\phi(\mathbf{u}, s)}{\int \mathrm{d}^3u \int \mathrm{d}s\, \xi(s)\mathrm{e}^{-u^2/2}}$$
$$= \frac{Eq\tau_0}{m}\frac{\int \mathrm{d}^3u \int \mathrm{d}s\, u_z H(\mathbf{u}, s; \tau_0\sqrt{T})}{\int \mathrm{d}^3u \int \mathrm{d}s\, \xi(s)\mathrm{e}^{-u^2/2}}$$
$$= \langle v_z \rangle_0 \frac{\int \mathrm{d}^3u \int \mathrm{d}s\, u_z H(\mathbf{u}, s; \tau_0\sqrt{T})}{\int \mathrm{d}^3u \int \mathrm{d}s\, \xi(s)\mathrm{e}^{-u^2/2}}.$$

Thus $\langle v_z \rangle/\langle v_z \rangle_0$ $(=\sigma/\sigma_0)$ depends on τ_0 only through the product $\tau_0\sqrt{T}$.

Figure 4 shows the variation of the conductivity as a fraction of the corresponding bulk value with wire radius, parametrized by τ_0. As τ_0 decreases, the results approach geometrically determinable values; further, as ω increases, not only does the geometrical factor move further below 1 but also the actual conductivity departs more and more from the geometrical value. Expectably, if the width is fixed, increasing the wire radius diminishes the strength of the surface effect.

The conformity with physical expectation and analytically known limits in the results above indicates the reliability of the numerical scheme and its suitability for other calculations based on the Boltzmann equation.

5. Limit of zero surface width

A simple parametrization of the surface in a zero-width surface model is provided by the 'specularity coefficient' ϵ, which is the non-zero probability of carriers incident on the surface
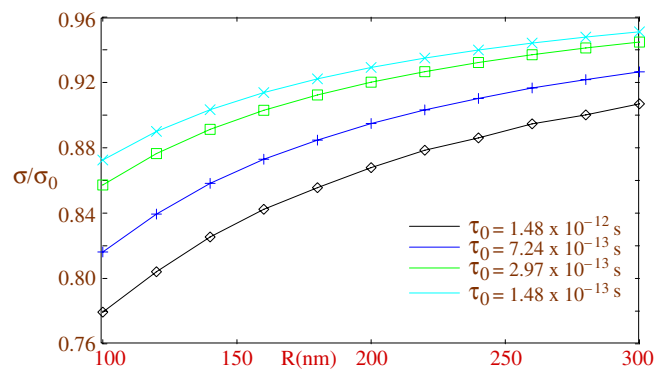
Figure 4. Relative conductivity as a function of wire radius. Here $E = 26 \text{ kV m}^{-1}$, $T = 300 \text{ K}$ and $w = 20 \text{ nm}$.
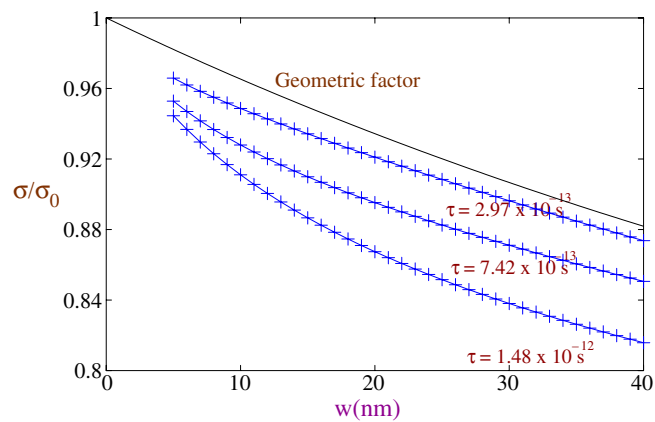

Figure 5. Variation of conductivity with surface width for different relaxation timescales. The geometric factor is included for reference. Here $E = 26 \text{ kV m}^{-1}$, $T = 300 \text{ K}$ and $R = 200 \text{ nm}$.

suffering a scattering event there: they undergo diffuse rather than specular reflection [46]. This is often encountered in the literature; for instance, it has also been used in the analogous context of thermal transport by phonons [47–50]. We now consider the physically important limit of $w \to 0$ which should relate the parameters in our model to the parameter ϵ. Figure 5 shows the numerical results obtained by varying the surface width parameter, along with the graph of the analytical geometric factor. Significantly, it is seen that even for large τ_0, the departure from the bulk value seems to go down to a small number, possibly zero. This is in contrast to [1] where the magnitude of the surface effect is unbounded as a function of the relaxation timescale or mean free path. It may be noted that the computation becomes increasingly more expensive, as the surface width is decreased; we believe that the lowest width used here is low enough to allow us to draw qualitative conclusions from the results.

We thus see an apparent contradiction between the results obtained with two different characterizations of the surface, which demands closer scrutiny. A direct contradiction results only if ϵ in the abrupt surface model is considered a free parameter assignable arbitrary values between 0 and 1; one could interpret the results we have seen as placing an upper limit on ϵ not far above zero. But this, on the other hand, would imply that such a parametrization is not very meaningful. Indeed, a value of $\epsilon = 1$ is assumed in [1].

The contrast between the two approaches becomes understandable when one recognizes the correlation between ϵ and the fraction of carriers resident within the surface layer. In a finite-width model, this fraction is always finite; it approaches zero only in the zero-width limit, when $\epsilon \to 0$. Equivalently, a non-zero value of ϵ is only compatible with the existence of a finite fraction of carriers on the surface. Thus if a finite-width model is accepted as more realistic, a value of ϵ close to 1 is physically possible only when a large part of the total number of carriers resides on the surface even in the absence of a field.

There is another way of pointing out the essential difference between an abrupt surface model and a finite-width one. In the former, it is assumed that a scattering at the surface necessarily returns the carrier into the bulk of the surface, whereas this is not the case in the latter, once again bringing to mind the existence of a finite surface population. Finally, in the former, there is no scale of the relaxation time at which the surface effect saturates, whereas, in the finite-width model, saturation occurs where the mean free path exceeds a few times the length scale ζ. Saturation is physically expected in the latter case—if, in some cases, typical carriers can sample regions with significantly different values of τ during a lifetime, any further increase of the lifetime should not make a big difference.

A future investigation of the surface effect resulting from a carrier distribution involving non-trivial features near the surface rather than the simple, monotonic decay studied here is expected to provide further insight. In particular, it may provide an explanation for the apparent experimental evidence [51] that ϵ is close to 1. In any case, the considerations stated in this section challenge the conception of the abrupt surface model, which ought to be reevaluated in the light of these numerical results.

6. Longitudinal magneto-conductance

The effect of a longitudinal magnetic field (B) on the conductivity of a large nanowire is of particular interest because the surface provides a classical kinetic mechanism for a magneto-resistive effect. In the large-field limit, one would expect the magnetic field to decouple different spatial regions by confining the carriers kinematically, constraining them to helical motion between collisions. Thus, when the cyclotron radius is smaller than ζ, the carriers are effectively localized by the magnetic field, so that the conductivity is largely determined by the geometric factor. As we have seen in section 4, the effect of spatial connectivity in a wire with a rough surface is to lower the conductivity below the geometric factor. Since a large B field ought to reduce connectivity, the magneto-conductance clearly ought to be positive. Further, this magneto-conductance is expected to saturate with B when the cyclotron radius for carriers with typical momentum values (around the thermal momentum p_{th}) becomes much smaller than ζ. On the other hand, the magnetic field has an appreciable effect only when the reciprocal of the cyclotron frequency for carriers with typical momenta is smaller than the relaxation time; the magnetic field is ineffective if the probability for a collision before the carrier velocity turns round once is high.

At intermediate values of B, it is not obvious whether there can be a case of negative magneto-conductance; the field could conceivably tend to produce a net movement of carriers in some regions down the gradient of $\tau(r)$. The results presented in figures 6 and 7 suggest that this does not occur; the magneto-conductance is seen to be positive within the accuracy of the calculation in all cases.

For relaxation times corresponding to the bulk mobility of a common semiconducting material like Si, the effect of the magnetic field is surprisingly small. In particular, the saturation values of B exceed realistic laboratory values, whereas the magnitude of the fractional magneto-conductance is still only a few per cent. Again, this is in contrast to the results in [1]. Although
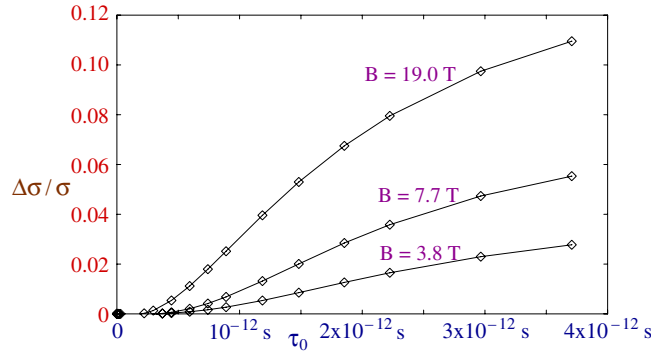
Figure 6. Fractional longitudinal magneto-conductance as a function of relaxation timescale for high magnetic fields. $E = 26 \, \text{kV m}^{-1}$, $T = 300 \, \text{K}$, $R = 200 \, \text{nm}$ and $w = 40 \, \text{nm}$.
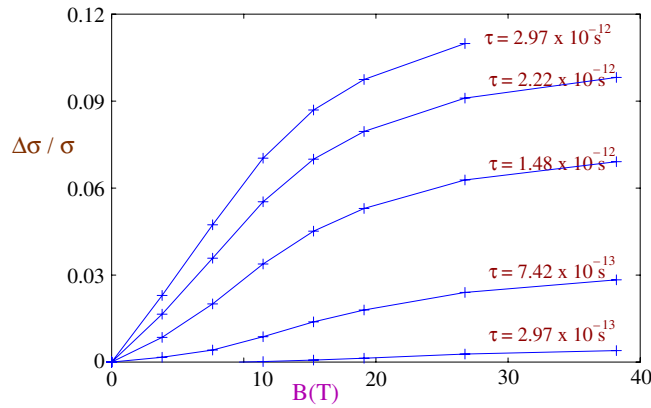

Figure 7. Variation of fractional magneto-conductance with B going up to very large values. The fixed parameters used are the same as in figure 6.

it is to be noted that the latter pertain to the degenerate limit (metallic case), the crux of the difference lies in the surface model, as argued in section 5. In short, if the surface effect is small, the magneto-conductive effect must also be limited by the corresponding departure from the geometric factor.

However, there still remains a qualitative similarity between our results and the results in [1]; for instance, we see that the low B results lend themselves to a good parabolic fit, which is consistent with [1]. Further, the arguments we have presented are substantiated by the fact that [1] systematically predicts a greater surface effect than the experimental results used for comparison, a discrepancy noted there itself. Since the discrepancy is despite the use of best-fit values, the parametrization itself must be regarded as dubious. It is important to note, however, that the results in [1] and our results are both consistent with recent experimental findings [28, 29, 31] to the extent that this surface magneto-resistive effect can be experimentally delineated from intrinsic quantum-mechanical effects.

The intriguing fact that the magnetic field increases conduction in all cases examined prompts a second look at the general effect of a spatially varying relaxation time. For one thing, using the same numerical scheme, we find another curious fact—the magneto-conductance does not flip sign when the profile of $\tau(r)$ is inverted, i.e. with a thin region of high mobility

surrounding a core of low mobility, even in the high B limit. More generally, we could not find a profile of $\tau(r)$ such as to yield a negative magneto-conductance.

We attribute the absence of a negative magneto-conductance to the asymmetry between smooth (high τ) and rough (low τ) regions in the effect of a spatial variation of τ, discussed in section 4. As explained there, the surface effect, which is the result of connectivity in the model at hand, tends to decrease the conductivity below the geometric value. Thus the introduction of a magnetic field, whose basic action is to undo the transport connection between different regions by confining carriers, in reversing the effect of connectivity, can only increase the conductivity.

One also sees, by the same line of reasoning, that the surface effect must be small if $\tau(r)$ is assumed to be continuous, since the region that contributes most to it is that where both τ and its gradient are large; but this region is of the order of the surface width w, which is expected to be small compared to the wire radius.

7. Conclusion

A direct solution of the Boltzmann transport equation offers a powerful approach to transport calculations in large nanowires. We have presented a simple finite-width model in a cylindrical geometry and shown that despite its simplicity, its scope is significantly greater than that of an abrupt surface model, from which it exhibits qualitative differences. This challenges the utility of an abrupt surface model, especially when parametrized by the specularity coefficient. Our numerical results show that the classical magneto-conductive effect in large nanowires of materials like Si is limited to a few per cent even with magnetic fields beyond the range of a practical laboratory set-up.

Acknowledgments

References

[1] Chambers R G 1950 *Proc. R. Soc.* A **202** 378
[2] Holmes J D, Johnston K P, Doty R C and Korgel B A 2000 *Science* **287** 1471
[3] Li C P, Sun X H, Wong N B, Lee C S and Teo B K 2002 *J. Phys. Chem.* B **106** 6980
[4] Sun Y, Yin Y, Mayers B T, Herricks T and Xia Y 2002 *Chem. Mater.* **14** 4736
[5] Hu S F, Wong W Z, Liu S S, Wu Y C, Sung C L and Huang T Y 2003 *Solid State Commun.* **125** 351
[6] Legrand B, Deresmes D and Stievenard D 2002 *J. Vac. Sci. Technol.* B **20** 862
[7] Duan X F, Huang Y, Cui Y, Wang J F and Lieber C M 2001 *Nature* **409** 66
[8] Cui Y, Lauhon L J, Gudiksen M S, Wang J F and Lieber C M 2001 *Appl. Phys. Lett.* **78** 2214
[9] Carim H, Lew K K and Redwing J 2001 *Adv. Mater.* **13** 1489
[10] Mbindyo J K N, Mallouk T E, Mattzela J B, Kratochvilova I, Razavi B, Jackson T N and Mayer T S 2002 *J. Am. Chem. Soc.* **124** 4020
[11] Cui Y, Zhong Z, Wang D, Wang W U and Lieber C M 2001 *Nano Lett.* **3** 149
[12] Cui Y and Lieber C M 2001 *Science* **291** 851
[13] Huang Y, Duan X, Wei Q and Lieber C M 2001 *Science* **291** 630
[14] Cui Y, Duan X, Hu J and Lieber C M 2000 *J. Phys. Chem.* B **104** 5213
[15] Chung S W, Yu J Y and Heath J R 2000 *Appl. Phys. Lett.* **76** 2068
[16] Yu J Y, Chung S W and Heath J R 2000 *J. Phys. Chem.* B **104** 11864
[17] Melosh N A, Boukai A, Diana F, Gerardot B, Badolato A, Petroff P M and Heath J R 2003 *Science* **300** 112
[18] Cui Y, Zhong Z, Wang D, Wang W U and Lieber C M 2003 *Nano Lett.* **3** 149
[19] Zhong Z, Qian F, Wang D and Lieber C M 2003 *Nano Lett.* **3** 343

[20] Gudiksen M S, Lauhon L J, Wang J, Smith D C and Lieber C M 2002 *Nature* **415** 617
[21] Huang Y, Duan X F, Lauhon L J, Kim K H and Lieber C M 2001 *Science* **294** 1313
[22] Muster J, Kim G T, Krstic V, Park J G, Park Y W, Roth S and Burghard M 2000 *Adv. Mater.* **12** 420
[23] Gu G, Burghard M, Kim G T, Dusberg G S, Chiu P W, Krstic V, Roth S and Han W Q 2001 *J. Appl. Phys.* **90** 5747
[24] Wang D W and Dai H J 2002 *Angew. Chem. Int. Edn Engl.* **41** 4783
[25] Shi W S, Zheng Y F, Wang N, Lee C S and Lee S T 2001 *J. Vac. Sci. Technol.* B **19** 1115
[26] Gates B, Mayers B, Grossman A and Xia Y 2002 *Adv. Mater.* **14** 1749
[27] Heremans J P, Thrush C M, Lin Y M, Cronin S B and Dresselhaus M S 2001 *Phys. Rev.* B **63** 085406
[28] Zhang Z B, Sun X, Dresselhaus M S, Ying J Y and Heremans J P 2000 *Phys. Rev.* B **61** 4850
[29] Lin Y, Cronin S B, Ying J Y, Dresselhaus M S and Heremans J P 2000 *Appl. Phys. Lett.* **76** 3944
[30] Zhang Z B, Gekhtman D, Dresselhaus M S and Ying J Y 1999 *Chem. Mater.* **11** 1659
[31] Liu K, Chien C L and Searson P C 1998 *Phys. Rev.* B **58** 14681
[32] Huber T E and Graf M J 1999 *Phys. Rev.* B **60** 16880
[33] Huber T E, Graf M J, Foss C A and Constant P 2000 *J. Mater. Res.* **15** 1816
[34] Lin Y M, Sun X and Dresselhaus M S 2000 *Phys. Rev.* B **62** 4610
[35] Sun X, Zhang Z and Dresselhaus M S 2000 *Appl. Phys. Lett.* **76** 3944
[36] Bjork M T, Ohlsson B J, Sass T, Persson A I, Thelander C, Magnusson M H, Deppert K, Wallenberg L R and Samuelson L 2002 *Appl. Phys. Lett.* **80** 1058
[37] Landman U, Barnett R N, Scherbakov A G and Avouris P 2000 *Phys. Rev. Lett.* **85** 1958
[38] Yeh C Y, Zhang S B and Zunger A 1994 *Phys. Rev.* B **50** 14405
[39] Dingle R B 1950 *Proc. R. Soc.* A **201** 545
[40] Cadet C, Deresmes D, Vuillaume D and Stievenard D 1994 *Appl. Phys. Lett.* **64** 2827
[41] Barthelemy A and Fert A 1991 *Phys. Rev.* B **43** 13124
[42] Erler F, Zahn P and Mertig I 2001 *Phys. Rev.* B **64** 094408
[43] Michez L A, Hickey B J, Shatz S and Wiser N 2003 *Phys. Rev.* B **67** 092402
[44] Visscher P B 1994 *Phys. Rev.* B **49** 3907
[45] Haug A 1972 *Theoretical Solid State Physics 46* vol 2, ed D Ter Haar (Oxford: Pergamon) pp 63–9
[46] Ziman J M 1960 *Electrons and Phonons* (Oxford: Clarendon) p 456
[47] Zou J and Balandin A 2001 *J. Appl. Phys.* **89** 2932
[48] Walkauskas S G, Broido D A, Kempa K and Reinecke T L 1999 *J. Appl. Phys.* **85** 2579
[49] Lu X and Chu J H 2002 *Eur. Phys. J.* B **26** 375
[50] Volz S G and Chen G 1999 *Appl. Phys. Lett.* **75** 2056
[51] Chambers R G 1950 *Nature* **165** 239